α clusters and collective flow in ultrarelativistic carbon–heavy-nucleus collisions

Piotr Bożek,[1,2,*] Wojciech Broniowski,[3,2,†] Enrique Ruiz Arriola,[4,‡] and Maciej Rybczyński[3,§]

[1]*AGH University of Science and Technology, Faculty of Physics and Applied Computer Science, al. Mickiewicza 30, 30-059 Krakow, Poland*
[2]*The H. Niewodniczański Institute of Nuclear Physics, Polish Academy of Sciences, PL-31342 Cracow, Poland*
[3]*Institute of Physics, Jan Kochanowski University, 25-406 Kielce, Poland*
[4]*Departamento de Física Atómica, Molecular y Nuclear and Instituto Carlos I de Física Teórica y Computacional,*
Universidad de Granada, E-18071 Granada, Spain

We investigate ultrarelativistic collisions of the ^{12}C nucleus with heavy targets and show that harmonic flow measures based on ratios of cumulant moments are particularly suited for study of the intrinsic deformation of the ^{12}C wave function. In this way one can probe the expected α clusterization in the ground state, which leads to a large initial triangularity in the shape of the fireball in the transverse plane. We show that the clusterization effect results in very characteristic behavior of the ratios of the cumulant moments as functions of the number of participant nucleons, for both elliptic and triangular deformations. Thus experimental event-by-event studies of harmonic flow in ultrarelativistic light-heavy collisions may offer a new window through which to look at the ground-state structure of light nuclei.

I. INTRODUCTION

In a recent paper [1] a novel method of investigating the α clusterization of light nuclei was proposed, exploring an unexpected bridge between the lowest-energy nuclear physics determining the ground-state structure and the highest-energy nuclear collisions. In this work we further pursue the method of searching for specific signals of the intrinsic geometry of light nuclei manifest in harmonic flow. Our approach is based on the fact that at ultrahigh collision energies, where nucleon-nucleon inelastic collisions generate a stream of copious particles, the interaction times are short enough to prevent the much slower nuclear excitations. Therefore, the initial spatial distributions of nucleons in the nuclear ground state of the overlying nuclei mark the locations of sources (inelastic collisions) igniting the fireball.

Atomic nuclei have a genuine degree of granularity which can be characterized by typical correlation lengths and which reflects the energetically favored spatial orderings. Any such geometric feature should leave some fingerprint in the final state, provided that these effects and the random fluctuations due to the finite number of particles can be cleanly separated. The theoretical identification and experimental verification of these geometry-preserving features not only would provide valuable information on conventional nuclear structure, where genuine multinucleon aspects of the nuclear wave functions could be tested, but also would generate confidence in the currently intricate theoretical protocols and approximation schemes used to analyze the dynamics of relativistic heavy-ion collisions.

In this paper we analyze in further detail the possible experimental signatures of the presence of α clusters in ^{12}C, which is of direct significance for analysis of its ultrarelativistic collisions with a heavy target. In particular, we focus on the ratios of harmonic flow measures investigated in the hydrodynamic framework [2] for the case of ^{3}He-Au collisions and defined in a suitable way such that the sensitivity to details of the intermediate dynamical/collective stages of the fireball evolution is eliminated. Such careful procedures are needed, as the studied observables carry information on both the initial geometry of the fireball and its random fluctuations, which have the tendency to cover up the geometry to some extent.

We show that the intrinsic triangular geometry of ^{12}C, predetermined by the arrangement of the α clusters, leads to a very specific and pronounced dependence of the considered measures on the number of nucleons participating in the collision. We argue that the proposed method provides practical tools to investigate signatures of the cluster structure of the ground-state wave function of light nuclei and that it could be directly employed in future studies of ultrarelativistic heavy-ion collisions in light-heavy systems.

The paper, designed for both researchers of α clusterization and the relativistic heavy-ion community, is arranged as follows: In Sec. II A we briefly review the current status of α clusterization in light nuclei, at the scope needed for our work. Based on this knowledge we prepare our nuclear Monte Carlo configurations of ^{12}C as described in Sec. II B. These configurations are later used in simulations of collisions with a heavy target.

Then we present our modeling of the early stage of the collision, stressing its quantum-mechanical aspects in Sec. III A. The important point here is that the reaction time at ultrarelativistic energies is much shorter than any typical nuclear-dynamics time, resulting in a frozen configuration of the nucleons reflecting the structure of the ground-state nuclear wave function. The formation of the fireball is described in Sec. III B, where we apply the popular Glauber approach [3–8] for our event-by-event studies. The key quantities here are the eccentricity parameters, defined in Sec. III C.

*Piotr.Bozek@ifj.edu.pl
†Wojciech.Broniowski@ifj.edu.pl
‡earriola@ugr.es
§Maciej.Rybczynski@ujk.edu.pl

In Sec. IV A we turn to harmonic flow—a phenomenon used extensively in relativistic heavy-ion programs to infer the properties of dynamically evolving quark-gluon plasma with the help of well-developed methods [9–12]. From our point of view, the essential feature here is the approximately linear response of the dynamical system to the eccentric deformation of the initial state, resulting in proportionality of the measurable flow coefficients to the corresponding initial eccentricity parameters. The unknown response coefficient may be eliminated by taking appropriate ratios of moments of the distribution, as explained in Sec. IV B. In particular, we consider moments based on two- and four-particle cumulants, used frequently in experimental studies. Such ratios for the flow moments are equal to the corresponding ratios for the eccentricity moments, thus allowing for predictions of the measured quantities related to flow based solely on measures of the initial state. Moreover, these ratios are sensitive to the geometry and random fluctuations in a very specific way.

In particular, we find that for ^{12}C collisions on a heavy target, the ratio of the four- to two-particle cumulant moments changes behavior for high-multiplicity events (centrality <10%), increasing with the number of participating nucleons for triangularity and decreasing for ellipticity, in accordance with the geometric features of the system. This is the key result of this work.

The feature holds at various collision energies (Sec. V A) and rapidities (Sec. V B), as well as for different Glauber models of the initial state (Sec. V D). We have also checked the dependence of our results on the model of the ^{12}C wave function (Sec. V D).

II. α CLUSTERS IN LIGHT NUCLEI

A. Overview

The idea of α clustering dates back to the old work of Gamow [13], where he conceived the radioactive α-decay process as a signal for nuclear constituents. This is in agreement with the tight binding ($B_\alpha/4 \sim 7$ MeV) and compactness ($r_\alpha \sim 1.5$ fm) of the quartet of states ($p \uparrow, p \downarrow, n \uparrow, n \downarrow$) building the ^{4}He nucleus and the weak $\alpha\alpha$ attraction ($V_{\alpha\alpha} \sim -2.5$ MeV) gluing the α particles into the light $A = 4n$ nucleus [14–16] (see, e.g., [17] for an early review and [18] for an historic account). This has been one of the most fascinating issues of nuclear structure physics throughout decades (for reviews of the topic see, e.g., [19–25]).

The ^{12}C nucleus is of particular interest. It was described as a bound state of three elementary α particles by Harrington [26] (for a review and further references see [27]). Numerous theoretical approaches were applied to its ground-state and excited-state structure: the Bose-Einstein condensation (BEC) model [28], fermionic molecular dynamics [29], antisymmetrized molecular dynamics [30], effective chiral field theory on the lattice [31], the no-core shell model [32,33], and the variational Green's function [variational Monte Carlo (VMC)] method [34]. The recently discovered 5^- rotational state of ^{12}C in low-energy $\alpha + {}^{12}$C collisions points to triangular $\mathcal{D}_{3h}$ symmetry of the system [35].

B. Generating clustered distributions

Our aim is to consider the α-clustered ground-state structure of ^{12}C. Ideally, distributions following from realistic model wave functions or *ab initio* calculations should be used. As this is quite involved, or requires access to the Monte Carlo nuclear configurations in the path-integral Green's function methods, we proceed in a simplified manner which grasps the essential features of the ground-state distributions and serves our purpose to sufficient accuracy. As we wish to study the effects of clusterization, we assume that ^{12}C is formed of three separated α clusters. The parameters of the arrangement are adjusted in such a way that the desired one-body radial density of the centers of nucleons is reproduced, as described below.

Technically, we carry out the Monte Carlo simulations of the nuclear configurations as follows: we place the centers of the three clusters in an equilateral triangle of edge length l. The distribution in each cluster is a Gaussian parametrized as

$$f_i(\vec{r}) = A \exp\left(-\tfrac{3}{2}(\vec{r} - \vec{c}_i)^2/r_\alpha^2\right), \tag{1}$$

where $\vec{r}$ is the coordinate of the nucleon, $\vec{c}_i$ is the position of the center of cluster i, and r_α is the rms radius of the cluster. We generate randomly the positions of the nucleons in sequence, alternating the number of the cluster—1, 2, 3, 1, 2, 3, etc.—and taking into account the short-distance NN repulsion in a simplified way, where the centers of each pair of nucleons cannot be closer than 0.9 fm [37]. At the end of the procedure the distributions are shifted such that their center of mass is placed at the origin of the coordinate frame. As a result, we get the Monte Carlo ^{12}C distributions with the built-in α-cluster correlations.

The model parameters l and r_α are optimized in such a way that the desired form of the radial density is approximately obtained. Thus the radial density of the centers of nucleons serves as a constraint for building the clustered distributions. Throughout this paper we use two reference radial distributions: those obtained from the so-called BEC model [28] and distributions from the VMC calculations using the Argonne v18 two-nucleon and Urbana X three-nucleon potentials, as recently provided at http://www.phy.anl.gov/theory/research/density. Figure 1 shows the quality of our fit to the one-body densities for the two considered cases—BEC in Fig. 1(a) and VMC in Fig. 1(b)—where we also give for a reference the result of the Jastrow-type correlated wave function [38].

The parameters used in our simulations are listed in Table I. As l is much larger than r_α, the distributions are hollow in the center, and the curves in Fig. 1 exhibit a dip, more depleted as r_α/l decreases. We note that, after properly implementing the nucleon charge contribution with $r_N = 0.87$ fm, the BEC densities reproduce very well the charge form factor of ^{12}C, which is not the case for the VMC, albeit the charge density near the origin carries rather large uncertainties inherited from the lack of knowledge in the high-momentum region in the measured charge form factor. As the BEC case is more strongly clustered than the VMC case (r_α/l is smaller), we use it as our basic model to illustrate the investigated effects, which are stronger with this choice. We occasionally make comparisons also to the VMC scenario.
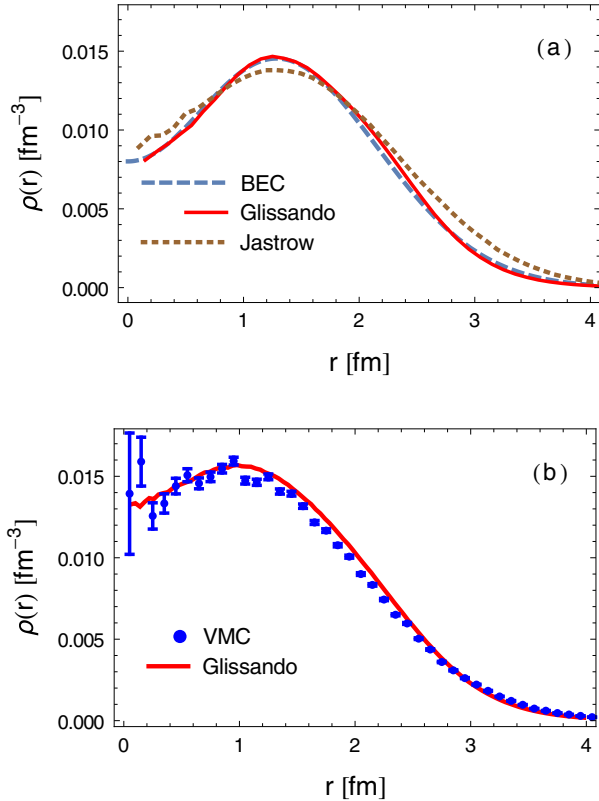
FIG. 1. (Color online) (a) Radial distribution of the centers of nucleons in ^{12}C for the BEC calculation reproducing the charge form factor (dashed line), our parametrization of the BEC calculation (solid line), and the Jastrow calculation in Ref. [36] (dotted line). (b) VMC calculation (points) and our parametrization (solid line). See text for details.

As we are interested in specific effects of clusterization, as a "null result" we also use the *uniform* distributions, i.e., with no α clusters. We prepare such distributions with exactly the same radial density as the clustered ones. This is achieved easily with a trick, where we randomly regenerate the spherical angles of the nucleons from the clustered distributions, while leaving the radial coordinate intact.

While the above-described procedure may seem crude for description of the nuclear structure, it is sufficient for our goal. We note that the method reproduces not only the one-body densities, as shown above, but also the two-particle densities determined from multicluster models with the state-dependent Jastrow correlations [38] with a reasonable accuracy (∼10%–20%), as shown in Fig. 2 [39].

TABLE I. Parameters used in our Monte Carlo simulations for the distributions of nucleons in ^{12}C.

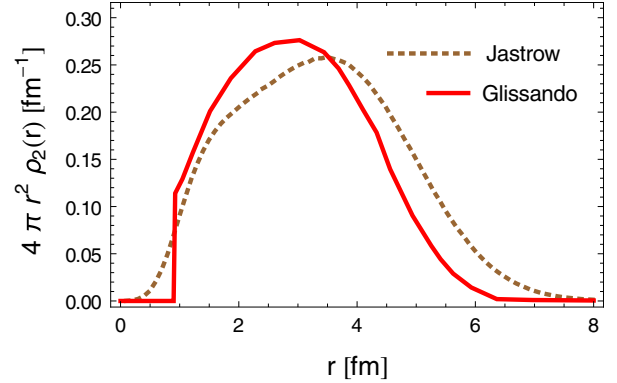| Parameter	BEC	VMC
l (fm)	3.05	2.84
r_α (fm)	0.96	1.15

FIG. 2. (Color online) Two-particle distribution $\rho_2(r)$ in ^{12}C, where r is the distance between the centers of nucleons in the pair. Solid line, GLISSANDO (BEC case); dashed line, Jastrow correlated wave function from Ref. [38].

III. EARLY STAGE OF THE ULTRARELATIVISTIC REACTION

A. Quantum-mechanical aspects of the collision

Viewed in the laboratory frame of collider experiments, colliding ultrarelativistic nuclei move at almost the speed of light. The corresponding Lorentz contraction factors are very large (∼1000 at LHC and ∼100 at RHIC energies), such that we deal with collisions of "flat pancakes" and hence the initial-state interactions are negligible; the reaction time is much shorter than any typical and slow nuclear structure time scale to witness any relevant nuclear excitation. As a result, in the reaction, a frozen nuclear ground-state configuration is seen. The wave function undergoes quantum-mechanical reduction in the earliest stage of the reaction, which results in a given intrinsic nuclear configuration. As outlined above, we generate the event-by-event probability following the square of the nucleus wave function.

The heavy nucleus which collides with ^{12}C (here ^{197}Au or ^{208}Pb) is made according to the Monte Carlo procedure described in detail [40,41]. Short-distance NN repulsion and nuclear deformation effects are taken into account.

Note that since ^{12}C is much smaller than ^{197}Au or ^{208}Pb, for sufficiently small impact parameters the collisions correspond to the α-clustered, triangle-shaped, and randomly oriented nucleus bumping into the central region of a heavy nucleus. This can pictorially be idealized as an equilateral triangle of three α's *hitting a wall* of nuclear matter.

In the following we are concerned with the transverse plane, relevant for the midrapidity physics studied later, hence we only need the wave functions in the transverse plane and midrapidity. The typical locations of the centers of ^{12}C nucleons are indicated by small diamonds in Fig. 3.

B. Formation of the fireball

The initial density of the fireball in ultrarelativistic heavy-ion collisions is formed from the individual NN collisions between nucleons from the two colliding nuclei. At these high energies most collisions are inelastic and copious particles
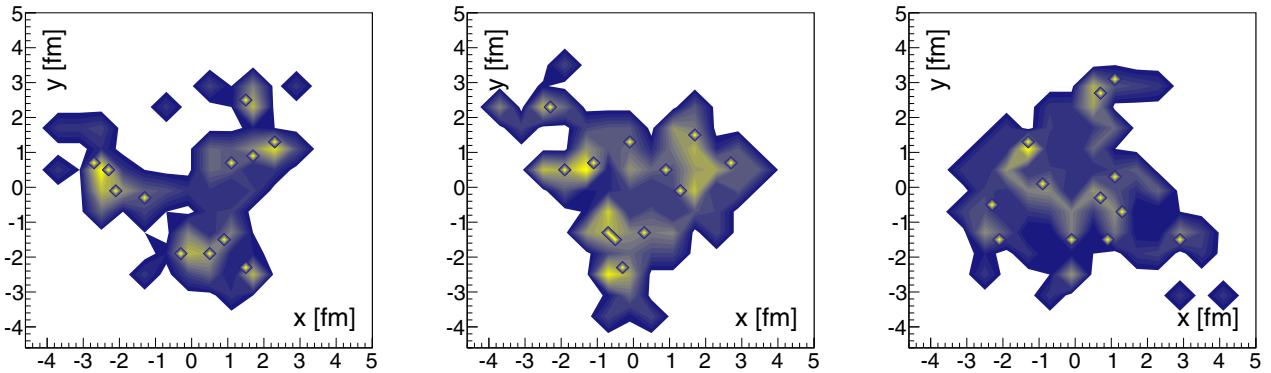
FIG. 3. (Color online) Snapshots of three sample ^{12}C–^{197}Au events, displaying the distribution of sources in the transverse plane. Small diamonds indicate the positions of the ^{12}C nucleons, while the dark (blue) region shows the density of the fireball including the wounded nucleons from ^{197}Au and the binary collisions. BEC case, RHIC, $N_w = 66$. In this simulation the transverse and cluster planes were aligned for better visualization. See text for details.

(partons) are produced. Popular modeling of this phase is accomplished with the Glauber approach [3–8], applied in this work. One may alternatively adopt the Kharzeev-Levin-Nardi framework [42–44] based on the color glass condensate model, which rests explicitly on quark-gluon dynamics (see, e.g., [45]).

Within the Glauber framework, we use the so-called mixed model [42,46], where the entropy deposition in the transverse plane comes from wounded nucleons [5], defined as those that interacted inelastically at least once, and from binary collisions. A source coming from the wounded nucleon is placed at its center with a relative weight $(1 − a)/2$, while the location of the binary collision is in the center of mass of the colliding nucleon pair, and the relative weight is a. The probability of the collision is defined relative to the total inelastic NN cross section, σ_{NN}^{inel}, corresponding to the center-of-mass collision energy in the process. The NN collision profile corresponds to the probability of the occurrence of an NN inelastic collision at a given impact parameter b. We use the smooth function described in Refs. [40,41], which is constructed to reproduce approximately the differential elastic NN cross section. The values of parameters used in our simulations are listed in Table II.

The Monte Carlo simulation produces, in each event, the location of the centers of the sources distributed in the transverse plane. Physically, sources generated in a collision process are of nonzero width, reflecting the production mechanism (nonzero size of nucleons, flux tubes, etc.), and thus the sources must be *smeared*. This feature can be modeled by placing a two-dimensional Gaussian of width σ (in this paper we take $\sigma = 0.4$ fm) centered at the source in the transverse plane. This *physical* smearing effect is necessary to form the initial

condition for hydrodynamics, taking over the evolution of the system. Also, smearing is phenomenologically important for shape eccentricities, which are significantly reduced compared to the naive evaluation with point-like sources. This smearing length sets a typical coarse-graining scale for hydrodynamics beyond which the integration step would not explore the relevant physics.

Sample events of a central ^{12}C–^{197}Au collision are presented in Fig. 3. We have used here the clustered ^{12}C BEC distributions and, for the purpose of better visibility, aligned the transverse and the cluster planes (the carbon hits the lead "flat"). Small diamonds represent the positions of the ^{12}C nucleons, while the dark (blue) region represents the transverse density of the fireball, including the wounded nucleons from ^{197}Au and the binary collisions. The irregular "warped" structure follows from the stochastic nature of the process. Nevertheless, one may easily note the remnant triangular shape in the fireball distribution, originating from the underlying three α clusters in ^{12}C.

C. Eccentricities of the initial state

With the smeared sources, the eccentricity parameters of the fireball, ϵ_n, are defined in each event via the Fourier decomposition of the density in the transverse plane,

$$\epsilon_n e^{in\Phi_n} = -\frac{\int dx\,dy\, f(x,y)\rho^n e^{in\phi}}{\int dx\,dy\, f(x,y)\rho^n}, \qquad (2)$$

where $n = 2,3, \ldots$ is the rank, Φ_n is the angle of the principal axes, x and y are coordinates in the transverse plane, with $\rho = \sqrt{x^2 + y^2}$ and $\tan\phi = y/x$, and, finally, $f(x,y)$ is the fireball density in the given event. The $n = 2$ eccentricity is termed *ellipticity*; the $n = 3$, *triangularity*.

Nonvanishing contributions to the coefficients ϵ_n come from two origins. One of them is the intrinsic "geometry" of the distribution of the nucleons in ^{12}C. In the clustered case there is a large triangularity of this distribution from the arrangement of the α clusters in an equilateral triangle. Although it is somewhat reduced due to the random orientation of the ^{12}C nucleus with respect to the transverse plane, the values of ϵ_3 remain sizable. The ^{12}C nucleus also exhibits

TABLE II. Parameters used in the GLISSANDO simulations.

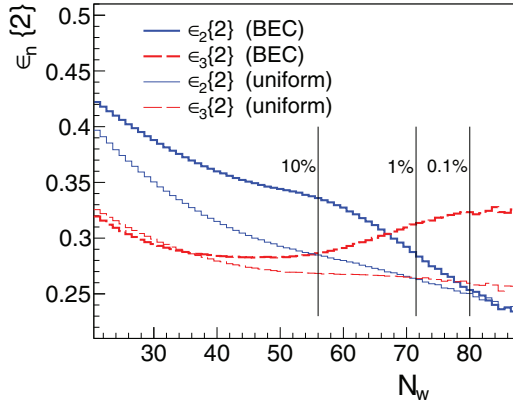|	System	$\sqrt{s_{NN}}$ (GeV)	σ_{NN}^{inel} (mb)	a
SPS	^{12}C $+$ ^{208}Pb	17	32	0.12
RHIC	^{12}C $+$ ^{197}Au	200	42	0.145
LHC	^{12}C $+$ ^{208}Pb	5200	73	0.15

FIG. 4. (Color online) Comparison of the fireball eccentricity coefficients from the two-particle cumulants for the clustered distribution and for the uniform distribution. GLISSANDO simulations, BEC case, RHIC. Vertical lines indicate the total number of wounded nucleons corresponding to centralities 10%, 1%, and 0.1%. The orientation-multiplicity correlation is clearly shown for the clustered case.

geometric ellipticity in the case where the cluster plane is not parallel to the transverse plane, which is the generic case due to randomness of the orientation.

The second cause for eccentricity coefficients comes from fluctuations due to the finite number of nucleons [7,47–50]. The effect of fluctuations washes away, to some extent, the geometric component, hence a careful examination of the results presented in Sec. IV B is necessary to discriminate the two origins.

In collisions of asymmetric nuclei at a finite impact parameter b, small values of odd Fourier components can appear in the azimuthal dependence of the fireball density with respect to the reaction plane (such an effect is present, for instance, in Cu-Au collisions). In Fig. 5 we show the triangularity of the initial fireball for C-Au and Cu-Au collisions with respect to the reaction plane calculated in the optical Glauber model, an approximate scheme where one first averages the densities and then computes the nuclear thickness function [51]. For intermediate values of b the triangularity is nonzero, even without any contribution from fluctuations or the α clustering. However, the obtained value of ϵ_3 is an order of magnitude smaller than the one calculated event by event with respect to the third-order event plane (Fig. 4). Moreover, the most central collisions that we discuss in the following correspond to small impact parameters (for centralities $c = 10\%$, 1%, and 0.1% the average values of b are 2.4, 1.5, and 1.2 fm, respectively). Hence the average geometric ϵ_3 in the reaction plane is even smaller. While the above effect is automatically included in our simulation, it does not play a role in the interpretation of the results.

As explained in Ref. [1], there is a specific correlation among centrality, triangularity, and ellipticity, induced by the intrinsic orientation of ^{12}C. When the transverse and the cluster planes are aligned, the ^{12}C nucleus hits the large nucleus flat-on and thus creates the most damage, i.e., produces the largest number of sources (cf. left side of Fig. 6). At the
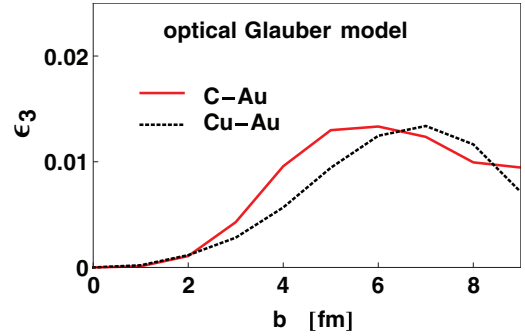

FIG. 5. (Color online) Triangularity of the fireball formed in C-Au and Cu-Au collisions. The density is calculated in the optical Glauber model, and the the triangularity is defined with respect to the reaction plane.

same time, in this flat-on orientation we have, on average, the highest triangularity and the lowest ellipticity, which here comes entirely from fluctuations.

In the other extreme case the cluster plane is perpendicular to the transverse plane (side-wise configuration; cf. right side of Fig. 6). Then we find the opposite behavior: low multiplicity, as the cross section is smaller, small triangularity, and large ellipticity, which now obtains a sizable contribution from the elongated shape of the fireball.

Of course, in actual collisions the orientation is random and we have a situation between the two limiting cases described above, yet the phenomenon of the specific orientation-multiplicity correlations is clearly seen (cf. Fig. 3, top right, in Ref. [1] or Fig. 4 here). In particular, in Fig. 4 we show, by comparing the simulations with clustered and uniform ^{12}C, that the geometry increases the triangularity at high values of the number of wounded nucleons, N_w (preferentially flat-on collisions), and raises ellipticity at lower values of N_w (sidewise collisions).

Event-by-event studies allow for obtaining event-by-event distributions of the physical quantities. In the sections below we need the so-called two-particle and four-particle cumulant moments [52] of the eccentricities, defined as

$$\epsilon_n\{2\} = \langle \epsilon_2^2 \rangle^{1/2},$$
$$\epsilon_n\{4\} = 2\left(\langle \epsilon_n^2 \rangle^2 - \langle \epsilon_n^4 \rangle\right)^{1/4}. \tag{3}$$

For a finite number of sources (wounded nucleons), even without geometric deformation, one has just from fluctuations $\epsilon_n\{m\} \neq 0$ for $m \geqslant 4$, with $\epsilon_n\{m\}$ decreasing as $1/N_w^{1-1/m}$ [50,53].
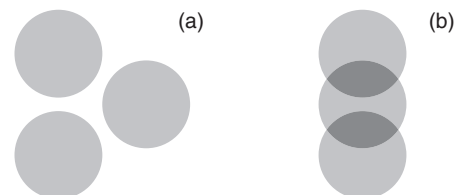

FIG. 6. Flat-on (left) and sidewise (right) orientations of ^{12}C with respect to the reaction plane.

IV. COLLECTIVITY AND DEVELOPMENT OF HARMONIC FLOW

A. Flow coefficients

The eccentricity coefficients described in the previous section are not directly observable, as they correspond to the stage right after one nucleus impinges on the other. In a hydrodynamic approach this is just the initial stage, whereas what one measures are the harmonic flow coefficients v_n, defined as the Fourier coefficients of the azimuthal dependence of the particle spectra, namely,

$$\frac{dN}{d\phi} = \frac{N}{2\pi}\left[1 + 2\sum_n v_n \cos[n(\phi - \Psi_n)]\right] \quad (4)$$

(here we consider the v_n coefficients integrated over the transverse momentum).

Realistic modeling of the flow coefficients requires advanced simulations of all stages of the reaction, from the early phase, through the intermediate hydrodynamics (for reviews see, e.g., [54,55], and references therein) or transport [56], to hadronization at freeze-out (see, e.g., [51] for a review). Such event-by-event simulations have been carried out for numerous reactions, displaying collectivity even for such small systems as in d-Au and p-Pb collisions [57–62].

A crucial finding with our method is that, to a very good accuracy, the flow coefficients are proportional to the initial eccentricity coefficients [63,64],

$$v_n = \kappa_n \epsilon_n, \quad n = 2,3. \quad (5)$$

The response coefficients κ_n depend on the details of the system and model (collision energy, multiplicity, viscosity of quark-gluon plasma, initial time of collective evolution, freeze-out temperature, feature of the applied "afterburner"), yet the linearity of Eq. (5) allows for model-independent studies for certain quantities as shown in the following sections. These relations, realizing the shape-flow transmutation phenomenon, buttress quantitatively the naive expectation of geometry-preserving features addressed in Sec. I.

We have carried out hydrodynamic simulations for the studied case of ^{12}C–^{197}Au collisions at RHIC energies. We have used the event-by-event $(3 + 1)$–dimensional viscous hydrodynamics of Ref. [65]. At the freeze-out temperature of 150 MeV hadrons are emitted following the statistical hadronization model [66,67]. The hydrodynamic evolution and particle emission at freeze-out include effects of the shear viscosity with $\eta/s = 0.08$ and the bulk viscosity with $\zeta = 0.04$ [68]. In Fig. 7 we present the obtained estimates for the elliptic $v_2\{2\}$ and triangular $v_3\{2\}$ (all charged hadrons, $150 \text{ MeV} < p_\perp < 2 \text{ GeV}$, $|\eta| < 1$) flow coefficients for two cases: the clustered and the uniform initial ^{12}C configurations. It is not possible to obtain directly accurate estimates of the higher-order cumulants $v_n\{4\}$ and $v_n\{6\}$ due to prohibitive requirements on the event-by-event statistics.

Our simulations confirm the approximate linearity of Eq. (5). The resulting response coefficients are presented in Fig. 8. We note that the response coefficients grow with N_w. The relative growth is quite strong; in particular, κ_3 increases by 50%, from $N_w = 30$ to $N_w = 80$.
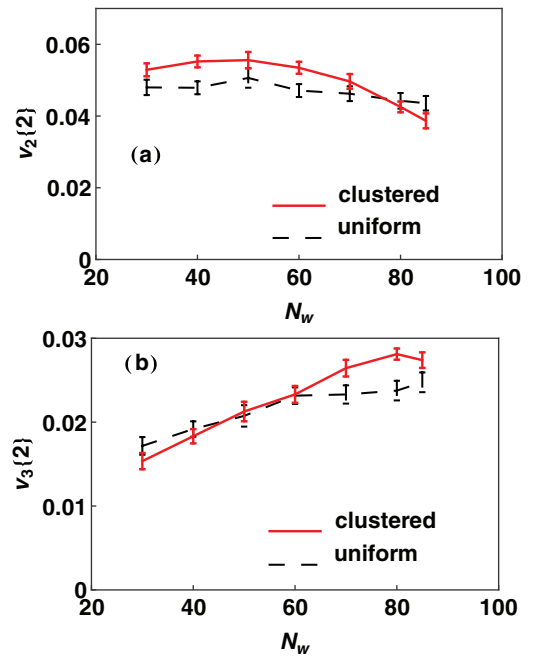

FIG. 7. (Color online) Elliptic (a) and triangular (b) flow coefficients as a function of the number of wounded nucleons for C-Au collisions, calculated using the second-order cumulant.

B. Ratios of flow coefficients

The above-mentioned increase in the response coefficient with multiplicity poses an obstacle in qualitative analyses of the clusterization effect. Imagine that the experiment finds a growth of triangularity with N_w. A priori, without detailed knowledge of the structure of the initial state and details of the dynamics, we cannot say how much of this growth should be attributed to intrinsic geometric deformation and how much comes from the enhanced hydrodynamic response. One may avoid this difficulty by taking ratios of moments of event-by-event distributions of ϵ_n which are independent of κ_n. Thanks to the proportionality, (5), the same relations hold for the moments of v_n. Two popular choices with low-order
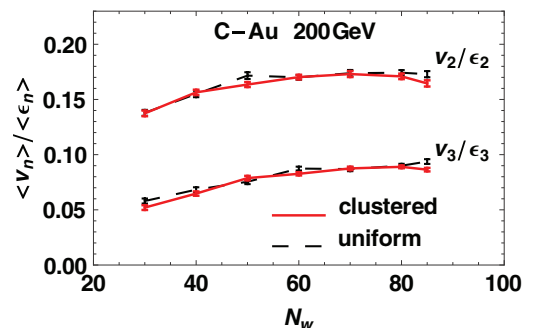

FIG. 8. (Color online) Hydrodynamic response coefficients for ellipticity and triangularity plotted as functions of the total number of wounded nucleons. BEC case, RHIC, $(3 + 1)$–dimensional viscous hydrodynamics.
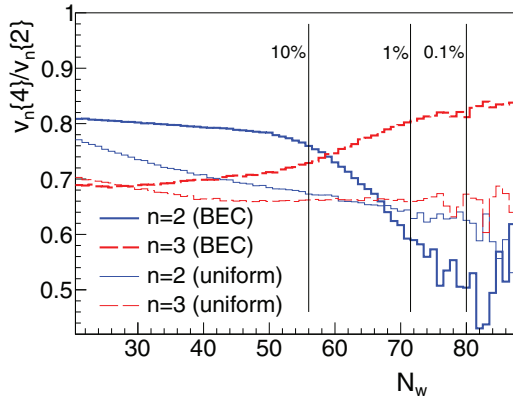
FIG. 9. (Color online) Ratios of four-particle to two-particle cumulants plotted as functions of the total number of wounded nucleons. BEC case, RHIC.
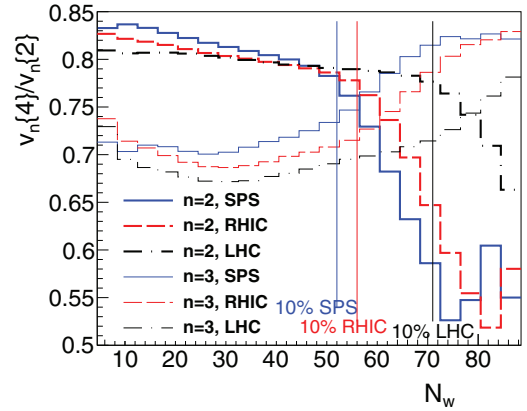

FIG. 10. (Color online) Comparison of $v_n\{4\}/v_n\{2\}$ for the SPS, RHIC, and LHC cases. BEC case. Vertical lines indicate the values of N_w corresponding to centralities of 10% for the three collision energies. Parameters are listed in Table II.

moments are the scaled standard deviation,

$$\frac{\sigma(\epsilon_n)}{\langle\epsilon_n\rangle} \simeq \frac{\sigma(v_n)}{\langle v_n\rangle}, \tag{6}$$

and the ratio of the four-particle and two-particle cumulant moments,

$$\frac{\epsilon_n\{4\}}{\epsilon_n\{2\}} \simeq \frac{v_n\{4\}}{v_n\{2\}}. \tag{7}$$

Thus measurements of the above combinations of moments of v_n provide information on analogous quantities for the eccentricities. Experimentally, one can access even moments of v_n, and the ratio in Eq. (6) must be estimated from $v_n\{2\}$ and $v_n\{4\}$ or from the reconstructed v_n distribution.

Predictions based on Eq. (6) have been reported in Ref. [1] (Fig. 3, top right, in that work), where $\sigma(\epsilon_n)/\langle\epsilon_n\rangle$ increases for ellipticity and decreases for triangularity with N_w. This behavior reflects the interplay of the intrinsic geometry and statistical fluctuations. In this paper, following closely the analysis in Ref. [2], we apply relation (7). The results of GLISSANDO simulations are shown in Fig. 9. We note that for high-multiplicity collisions the ratio $\epsilon_n\{4\}/\epsilon_n\{2\}$ significantly increases for triangularity and decreases for ellipticity. The geometric triangularity increases for collisions with a larger number of participants, corresponding to high-multiplicity events. On the other hand, the eccentricity due to fluctuations of independent sources decreases with N_w, hence the opposite behavior.

We note that the change of behavior (stronger monotonicity) starts at N_w, corresponding to a centrality of 10%; thus it occurs in the region easily accessible to experimental analyses. We also see that the behavior for clustered ^{12}C (thick lines in Fig. 9) is completely different from the case of the uniform structure (thin lines).

The behavior shown in Fig. 9 is the key result of this work. It offers a signature sensitive to the intrinsic deformation that is straightforward to measure in ultrarelativistic heavy-ion collisions with standard techniques devoted to analysis of harmonic flow.

One could ask at this point why we need to resort to Eq. (7), rather than evaluating $v_n\{4\}$ directly from the event-by-event hydrodynamic calculations. The reason is twofold. First, the statistics possible to achieve in such studies is sufficient for the analysis of two-particle cumulants but not four-particle cumulants. Second, and more importantly, the application of Eq. (7) frees us from sensitivity to details of the dynamical theory, which we do not know exactly. This way the predictions for the ratios of the cumulant moments are more general and model independent.

V. FURTHER RESULTS

A. Dependence on the collision energy

In Fig. 10 we show the dependence of our predictions on the collision energy, according to the values in Table II. We note that the qualitative predictions do not change with the collision energy, as the three sets of curves are similar, in particular, when we take into account the fact that the values of centrality corresponding to a given N_w depend on the energy via the value of σ_{NN}^{inel}.

B. Forward and backward rapidity

We may also ask the question how much the predictions depend on the rapidity window used in the experiment. This is of practical significance, as in fixed-target experiments the detectors cover rapidity away from the center. For the purpose of a simple estimate, we use the model in Refs. [69,70], where the initial density of the fireball in the space-time rapidity $\eta_\parallel$ and the transverse plane coordinates (x, y) is given by the form

$$F(\eta_\parallel, x, y) = (1 - a)[\rho_+(x, y)f_+(\eta_\parallel) + \rho_-(x, y)f_-(\eta_\parallel)]$$
$$+ a\rho_{bin}(x, y)[f_+(\eta_\parallel) + f_-(\eta_\parallel)], \tag{8}$$

where $\rho_\pm(x, y)$ is the density from the forward- and backward-going wounded nucleons, and $\rho_{bin}(x, y)$ is the binary collision density. The rapidity profile functions $f_+(\eta_\parallel)$ and $f_-(\eta_\parallel)$ are given explicitly in Ref. [70].
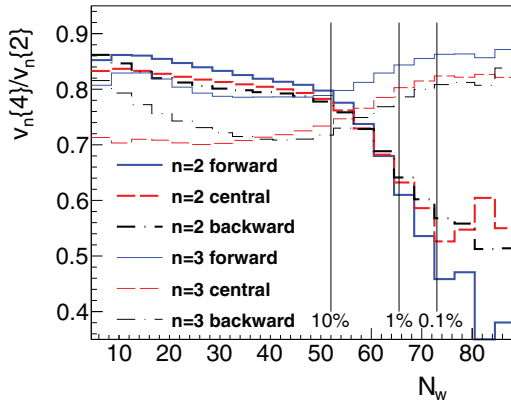
FIG. 11. (Color online) Ratios of four-particle to two-particle cumulants in the forward, central, and backward rapidity regions, plotted as functions of the total number of wounded nucleons. BEC case, SPS.

For our purpose it only matters that at midrapidity $f_\pm(0) = 1/2$, hence $F(0) = (1-a)\frac{1}{2}(\rho_+ + \rho_-) + a\rho_{bin}$, which is nothing but the density of the mixed model used up to now to evaluate the fireball eccentricities. At very forward rapidities η_+ the value of $f_-(\eta_+)$ is negligible compared to $f_+(\eta_+)$, hence the relevant density of the fireball is $F(\eta_+) = f_+(\eta_+)[(1-a)\rho_+ + a\rho_{bin}]$. Analogously, at large backward rapidities η_- we have $F(\eta_-) = f_-(\eta_-)[(1-a)\rho_- + a\rho_{bin}]$.

The results of the calculation using central, forward (i.e., the ^{12}C hemisphere), and backward rapidity windows, with the source density constructed according to the above-described prescription, are shown in Fig. 11. We note that the results are not altered much with the choice of rapidity. We can see that the forward case has the highest ratio for the triangularity, which follows from the fact that it is more sensitive to the distribution of nucleons in the clustered ^{12}C. However, the monotonic behavior is not very different, and there should not be much difference in the results obtained at midrapidity in colliders and at peripheral rapidity in fixed-target experiments.
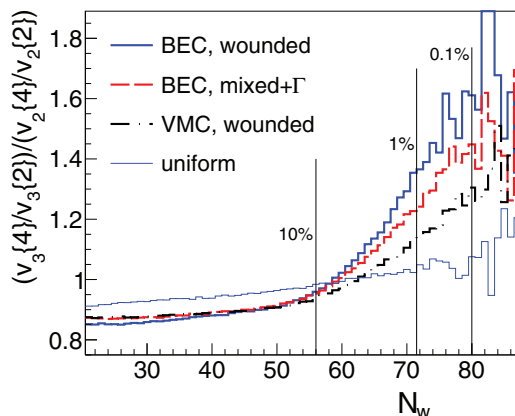

FIG. 12. (Color online) Comparison of the double ratio $(v_3\{4\}/v_3\{2\})/(v_2\{4\}/v_2\{2\})$ for various models, plotted as functions of the total number of wounded nucleons, RHIC.
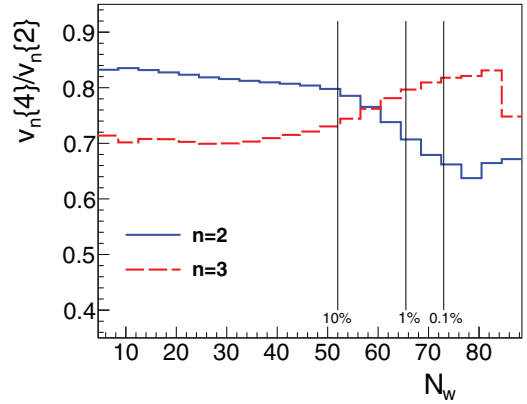

FIG. 13. (Color online) Predictions for $v_n\{4\}/v_n\{2\}$ for the ^{12}C distribution where α clusters are arranged in a deformed triangle, mimicking the fermionic molecular dynamics calculation in Ref. [29]. SPS case. See text for details.

C. Dependence on the model of the initial state

Up to now we have used the mixed model of the formation of the initial state and the BEC distribution in ^{12}C. In this subsection we study other variants of the Glauber approach, as well as the VMC distributions. The studied effects of clusterization depend to some extent on the models of the initial state, as they involve different amounts of fluctuation. They also obviously depend on the configuration of the ground state of ^{12}C. In Fig. 12 we present the double ratio $(v_3\{4\}/v_3\{2\})/(v_2\{4\}/v_2\{2\})$ for several cases.

We note the difference between the wounded nucleon model (less fluctuations) and the mixed model with the overlaid Γ distribution [40] (significantly more fluctuations). On the other hand, the result for the VMC distributions is, as expected from the discussion in Sec. II B, significantly weaker. This sensitivity is desired, as it, in principle, allows for a quantitative discrimination of the ^{12}C wave functions from studies of flow in ultrarelativistic collisions.

D. Deformed triangle

Finally, we study the case where the ^{12}C nucleus is formed by placing three α clusters in a deformed isosceles triangle, as results from the fermionic molecular dynamics studies in Ref. [29]. For that purpose we take the ratio of the length of the edges to be 3/4, the value that can be read off from the rightmost plot in Fig. 2 in Ref. [29].

The results of this calculation, displayed in Fig. 13, show that the qualitative behavior is the same as for the case of the equilateral triangle studied in the preceding sections.

VI. CONCLUSIONS

We have pursued the idea that there is a geometry-preserving principle operating in ultrarelativistic collisions, involving light nuclei impinging on heavy ions. The extremely high energies make the interaction time so short that the existing granular structures present in the ground-state nuclear wave function are effectively frozen. The collision process realizes a snapshot which may be recorded as a pattern in

the collective flow emerging from the abundantly produced particles in individual nucleon-nucleon inelastic collisions.

The presence of fluctuations due to the finite number of particles as well the limitations imposed by the finite nuclear size causes the geometric signals to be generically blurred by random fluctuations. For that reason a careful analysis, as described in this paper, must be carried out.

We have addressed the question of the intrinsic triangularity structure of ^{12}C motivated by the ancient idea that it has a cluster structure, with the three α particles sitting at the corners of an equilateral triangle, and the fact that the 12 nucleons induce a sufficiently large collectivity when colliding with heavy ions such as ^{197}Au and ^{208}Pb. Other light isotopes in the region $A \sim 10$ may undergo a study similar to the one conducted here.

Furthermore, our analysis is insensitive to the hydrodynamic details, as it relies on the linear response of the harmonic flow to the initial conditions. For this purpose, we examine the ratios of cumulant moments, which are very well suited for our strategy. We find that visible signals are expected in the dependence of these ratios on the number of wounded nucleons, a feature which makes them particularly suitable for experimental analysis.

The fascinating possibility of catching the ^{12}C nucleus as a triangle of α particles in ultrarelativistic collisions would provide further evidence of Gamow's idea, taken from a different angle than traditionally expected, and could be discerned on experimental grounds. A positive answer would also generate further confidence in the currently intricate theoretical approaches.

[1] W. Broniowski and E. Ruiz Arriola, Phys. Rev. Lett. **112**, 112501 (2014).

[2] P. Bożek and W. Broniowski, Phys. Lett. B **739**, 308 (2014).

[3] R. J. Glauber, in *Lectures in Theoretical Physics*, edited by W. E. Brittin and L. G. Dunham (Interscience, New York, 1959), Vol. 1, p. 315.

[4] W. Czyż and L. Maximon, Ann. Phys. **52**, 59 (1969).

[5] A. Białas, M. Błeszyński, and W. Czyż, Nucl. Phys. **B111**, 461 (1976).

[6] M. L. Miller, K. Reygers, S. J. Sanders, and P. Steinberg, Annu. Rev. Nucl. Part. Sci. **57**, 205 (2007).

[7] W. Broniowski, P. Bożek, and M. Rybczyński, Phys. Rev. C **76**, 054905 (2007).

[8] A. Białas, J. Phys. G **35**, 044053 (2008).

[9] J.-Y. Ollitrault, Phys. Rev. D **46**, 229 (1992).

[10] N. Borghini, P. M. Dinh, and J.-Y. Ollitrault, Phys. Rev. C **64**, 054901 (2001).

[11] S. Voloshin, Nucl. Phys. **A715**, 379 (2003).

[12] S. A. Voloshin, A. M. Poskanzer, and R. Snellings, in *Landolt-Boernstein, Relativistic Heavy Ion Physics*, Vol. 1/23 (Springer-Verlag, Berlin, 2010), arXiv:0809.2949.

[13] G. Gamow, *Constitution of Atomic Nuclei and Radioactivity* (Oxford University Press, New York, 1931).

[14] J. A. Wheeler, Phys. Rev. **52**, 1083 (1937).

[15] L. R. Hafstad and E. Teller, Phys. Rev. **54**, 681 (1938).

[16] W. Wefelmeier, Z. Phys. **107**, 332 (1937).

[17] J. Blatt and V. Weisskopf, *Theoretical Nuclear Physics* (John Wiley and Sons, New York, 1952).

[18] D. Brink, in *Journal of Physics: Conference Series*, Vol. 111 (IOP, Washington, DC, 2008), p. 012001.

[19] D. Brink, *Proceedings International School Enrico Fermi, Course 36 (1965)*, edited by C. Bloch (Academic Press, New York, 1966), p. 247.

[20] M. Freer, Rep. Prog. Phys. **70**, 2149 (2007).

[21] K. Ikeda, T. Myo, K. Kato, and H. Toki, *Clusters in Nuclei*, Vol. 1 (Lecture Notes in Physics 818) (Springer, Berlin, 2010).

[22] C. Beck, *Clusters in Nuclei*, Vol. 2 (Lecture Notes in Physics 848) (Springer, Berlin, 2012).

[23] J. Okołowicz, W. Nazarewicz, and M. Płoszajczak, Fortsch. Phys. **61**, 66 (2013).

[24] P. I. Zarubin, *Clusters in Nuclei*, Vol. 3 (Springer, Berlin, 2014).

[25] C. Beck, arXiv:1408.0684 [nucl-ex].

[26] D. R. Harrington, Phys. Rev. **147**, 685 (1966).

[27] M. Freer and H. Fynbo, Prog. Part. Nucl. Phys. **78**, 1 (2014).

[28] Y. Funaki, A. Tohsaki, H. Horiuchi, P. Schuck, and G. Röpke, Eur. Phys. J. A **28**, 259 (2006).

[29] M. Chernykh, H. Feldmeier, T. Neff, P. von Neumann-Cosel, and A. Richter, Phys. Rev. Lett. **98**, 032501 (2007).

[30] Y. Kanada-En'yo, Prog. Theor. Phys. **117**, 655 (2007).

[31] E. Epelbaum, H. Krebs, T. A. Lahde, D. Lee, and U.-G. Meissner, Phys. Rev. Lett. **109**, 252501 (2012).

[32] R. Roth, S. Binder, K. Vobig, A. Calci, J. Langhammer, and P. Navratil, Phys. Rev. Lett. **109**, 052501 (2012).

[33] B. R. Barrett, P. Navratil, and J. P. Vary, Prog. Part. Nucl. Phys. **69**, 131 (2013).

[34] S. C. Pieper, K. Varga, and R. B. Wiringa, Phys. Rev. C **66**, 044310 (2002).

[35] D. Marin-Lambarri, R. Bijker, M. Freer, M. Gai, T. Kokalova, D. J. Parker, and C. Wheldon, Phys. Rev. Lett. **113**, 012502 (2014).

[36] E. Buendía, F. Gálvez, J. Praena, and A. Sarsa, J. Phys. G **27**, 2211 (2001).

[37] W. Broniowski and M. Rybczyński, Phys. Rev. C **81**, 064909 (2010).

[38] E. Buendia, F. J. Galvez, and A. Sarsa, Phys. Rev. C **70**, 054315 (2004).

[39] W. Broniowski and E. Ruiz Arriola, arXiv:1407.8495 [nucl-th].

[40] W. Broniowski, M. Rybczyński, and P. Bożek, Comput. Phys. Commun. **180**, 69 (2009).

[41] M. Rybczyński, G. Stefanek, W. Broniowski, and P. Bożek, Comput. Phys. Commun. **185**, 1759 (2014).

[42] D. Kharzeev and M. Nardi, Phys. Lett. **B507**, 121 (2001).

[43] D. Kharzeev, E. Levin, and M. Nardi, Nucl. Phys. **A730**, 448 (2004).

[44] A. Adil, H.-J. Drescher, A. Dumitru, A. Hayashigaki, and Y. Nara, Phys. Rev. C **74**, 044905 (2006).

[45] J. L. Albacete and C. Marquet, Prog. Part. Nucl. Phys. **76**, 1 (2014).

[46] B. Back *et al.* (PHOBOS Collaboration), Phys. Rev. C **65**, 031901 (2002).

[47] M. Miller and R. Snellings, arXiv:nucl-ex/0312008 [nucl-ex].

[48] S. Manly *et al.* (PHOBOS Collaboration), Nucl. Phys. **A774**, 523 (2006).

[49] S. A. Voloshin, arXiv:nucl-th/0606022 [nucl-th].

[50] B. Alver and G. Roland, Phys. Rev. C **81**, 054905 (2010).

[51] W. Florkowski, *Phenomenology of Ultra-relativistic Heavy-Ion Collisions* (World Scientific, Singapore, 2010).

[52] N. Borghini, P. M. Dinh, and J.-Y. Ollitrault, Phys. Rev. C **63**, 054906 (2001).

[53] R. S. Bhalerao and J.-Y. Ollitrault, Phys. Lett. **B641**, 260 (2006).

[54] U. Heinz and R. Snellings, Annu. Rev. Nucl. Part. Sci. **63**, 123 (2013).

[55] C. Gale, S. Jeon, and B. Schenke, Int. J. Mod. Phys. **A28**, 1340011 (2013).

[56] Z.-W. Lin, C. M. Ko, B.-A. Li, B. Zhang, and S. Pal, Phys. Rev. C **72**, 064901 (2005).

[57] P. Bożek, Phys. Rev. C **85**, 014911 (2012).

[58] A. Adare *et al.* (PHENIX Collaboration), Phys. Rev. Lett. **111**, 212301 (2013).

[59] A. M. Sickles (PHENIX Collaboration), arXiv:1310.4388 [nucl-ex].

[60] P. Bożek, W. Broniowski, and G. Torrieri, Phys. Rev. Lett. **111**, 172303 (2013).

[61] A. Bzdak, B. Schenke, P. Tribedy, and R. Venugopalan, Phys. Rev. C **87**, 064906 (2013).

[62] G.-Y. Qin and B. Müller, Phys. Rev. C **89**, 044902 (2014).

[63] F. G. Gardim, F. Grassi, M. Luzum, and J.-Y. Ollitrault, Phys. Rev. C **85**, 024908 (2012).

[64] H. Niemi, G. S. Denicol, H. Holopainen, and P. Huovinen, Phys. Rev. C **87**, 054901 (2013).

[65] P. Bożek, Phys. Rev. C **85**, 034901 (2012).

[66] A. Kisiel, T. Tałuć, W. Broniowski, and W. Florkowski, Comput. Phys. Commun. **174**, 669 (2006).

[67] M. Chojnacki, A. Kisiel, W. Florkowski, and W. Broniowski, Comput. Phys. Commun. **183**, 746 (2012).

[68] P. Bożek, Phys. Rev. C **81**, 034909 (2010).

[69] A. Białas and W. Czyż, Acta Phys. Polon. **B36**, 905 (2005).

[70] P. Bożek and I. Wyskiel, Phys. Rev. C **81**, 054902 (2010).